Article

Vestibular and active self-motion signals drive visual perception in binocular rivalry

ambiguous visual movement

stationary body

cyclical body rotation

visual percept:
stochastic

visual percept:
entrained to body rotation

David Alais,
Robert Keys, Frans
A.J. Verstraten,
Chris L.E. Paffen

david.alais@sydney.edu.au

Highlights

Binocular rivalry between left/right motions is stabilized by congruent head movement

Left/right head rotations entrain rivalry dynamics so matching direction is perceived

Active and passive rotations both drive rivalry dominance to match rotation direction

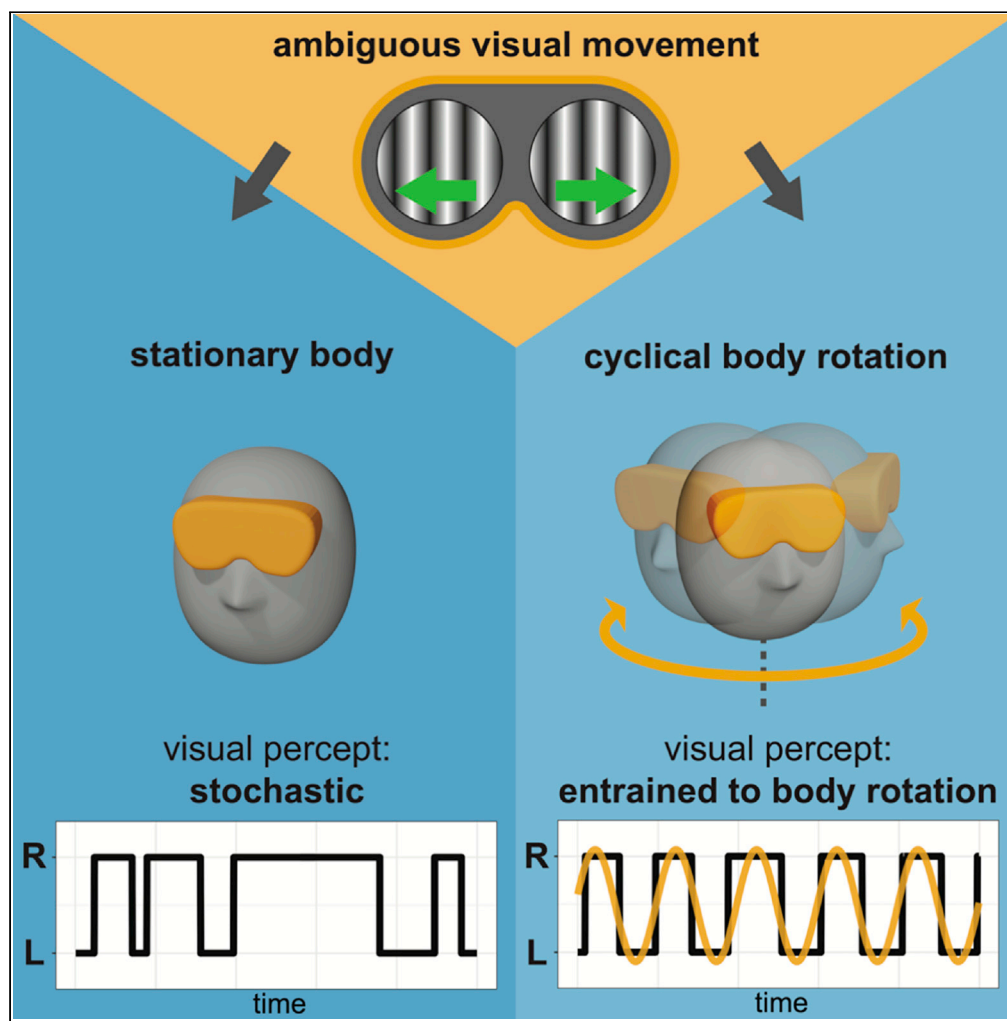Resolving ambiguous vision occurs in a broader vestibular and action-based context

Article

Vestibular and active self-motion signals drive visual perception in binocular rivalry

David Alais,[1,3,*] Robert Keys,[1] Frans A.J. Verstraten,[1] and Chris L.E. Paffen[2]

SUMMARY

Multisensory integration helps the brain build reliable models of the world and resolve ambiguities. Visual interactions with sound and touch are well established but vestibular influences on vision are less well studied. Here, we test the vestibular influence on vision using horizontally opposed motions presented one to each eye so that visual perception is unstable and alternates irregularly. Passive, whole-body rotations in the yaw plane stabilized visual alternations, with perceived direction oscillating congruently with rotation (leftward motion during leftward rotation, and *vice versa*). This demonstrates a purely vestibular signal can resolve ambiguous visual motion and determine visual perception. Active self-rotation following the same sinusoidal profile also entrained vision to the rotation cycle – more strongly and with a lesser time lag, likely because of efference copy and predictive internal models. Both experiments show that visual ambiguity provides an effective paradigm to reveal how vestibular and motor inputs can shape visual perception.

INTRODUCTION

Combining sensory information from visual and vestibular sources is critical for robust self-motion perception, gaze stabilization, spatial orientation, and postural control (Cullen, 2012). The strong influence of vision on vestibular processing is well established, with visual inputs modulating vestibular processing at all stages from the vestibular nucleus to cortical areas (Bremmer et al., 2002; Cullen, 2012; Lopez and Blanke, 2011). Consequently, vision can modulate vestibular function to produce dramatic behavioral and perceptual effects, such as induced body sway, subjective self-motion, and perceived self-rotation (Benson and Brown, 1989; Dichgans and Brandt, 1978). It is less clear whether vestibular self-motion signals would affect visual motion perception, and a convenient paradigm to study this is lacking. However, vestibular signals input to dorsal motion areas, primarily ventral intraparietal (VIP) (Bremmer et al., 2002; Schlack et al., 2002) and middle superior temporal (MST) where many neurons respond to combined visual and vestibular stimuli (Chen et al., 2013; Duffy, 1998). To test for vestibular modulation of visual motion, we adopted a sensitive method that exploits perceptual ambiguity to reveal non-visual signals modulating visual perception (Lunghi and Alais, 2013; Lunghi et al., 2014).

The method creates perceptual ambiguity by presenting incompatible monocular images to the eyes, preventing fusion, and triggering binocular rivalry (Alais and Blake, 2015; Blake and Logothetis, 2002) – an irregular sequence of perceptual switching (Alais, 2012) between each eye's input which cannot be resolved (Alais and Blake, 2005) and is not serially predictable (Blake et al., 1971; Fox and Herrmann, 1967). With two equiprobable visual stimuli balancing perception on a knife-edge, cross-modal inputs to vision can be revealed by studying switch dynamics. When a cross-modal stimulus congruent with one of the rivaling images causes perception to dwell on the congruent image, it indicates a clear and selective multisensory interaction. This paradigm has previously revealed tuned auditory (Conrad et al., 2010; Lunghi et al., 2014) and tactile (Hense et al., 2019; Lunghi et al., 2014; Lunghi and Alais, 2015) modulation of vision. For example, touching a tactile grating that is oriented to match one of a pair of rivaling visual gratings causes the matched grating to remain visible longer when it is perceptually dominant, in addition to shortening its suppression duration when suppressed (Lunghi and Alais, 2013). The effect is orientation-selective and reduces the strength of suppression exerted on the congruent grating during rivalry suppression (Lunghi and Alais, 2015).

Here, we test whether vestibular and active self-motion signals input to vision to influence binocular rivalry between opposed visual motions. We use a motion platform to rotate participants back and forth in the

[1]School of Psychology, The University of Sydney, Sydney, NSW 2006, Australia

[2]Department of Experimental Psychology & Helmholtz Institute, Utrecht University, 3584 CS Utrecht, the Netherlands

[3]Lead contact

*Correspondence: david.alais@sydney.edu.au

horizontal plane following a sinusoidal pattern while they view rivaling horizontal motions. Based on findings reviewed above that congruent stimuli in other modalities can exert a tuned disambiguating influence on visual rivalry, we expect that vestibular signals from the yaw rotation will influence rivalry dynamics by favoring dominance of the visual motion congruent with rotation. A second experiment uses active self-rotation instead of passive rotation and in both cases we find a strong and direction-selective influence of yaw rotation on motion rivalry, with active rotations exerting a stronger and less time-lagged influence.

RESULTS

In piloting these experiments, it became clear when participants underwent yaw-plane oscillations that perceptual alternations between rivaling horizontal motions tended to alternate cyclically with the physical rotation. For this reason, the following analyses focus on the strikingly cyclic nature of perceptual alternations we observed (see Figure 1A). To do so, the time course of rivalry alternations, which show how a participant's awareness switches between perceiving left and right directions over time, were fit with sinusoids. A strong prediction of cyclically entrained rivalry alternations is that the rivalry time course should conform to a sinusoid whose frequency matches the yaw rotation rate, and no other frequencies. The strength of rivalry's entrainment to rotation should be evident by the amplitude of the time course's sinusoidal pattern. Moreover, if participants' rivalry alternation time-courses can be described by a common frequency, the data can be further analyzed for phase to determine whether rivalry alternations lead or lag the rotation cycle, and by how much. These analyses are implemented in Experiments 1 and 2 which, respectively, examine how passive and active yaw rotation influence the dynamics of horizontal motion rivalry, as compared to vertical motion rivalry and stationary conditions as controls.

Experiment 1: passive whole-body yaw rotation

Figure 2A shows the mean rivalry alternation time course (averaged over eight trials) for one observer reporting perceived direction of horizontal motion rivalry while undergoing passive, whole-body yaw rotation (i.e., in the horizontal plane) at a rate of 0.25 Hz. The rivalry data pattern is well described by a sinusoid with best-fitting frequency very close to 0.25 Hz, matching the rate of passive rotation. To verify the sinusoidal fit to the time course and check for other prominent frequencies, we fitted sinusoids over a finely sampled range of interest (0.14–0.50 Hz; periods of 2–7 s), with amplitude and phase being free parameters at each frequency. Figure 2B plots goodness-of-fit (R^2) for the sinusoids fitted at each point in the sampled frequency range for the same observer (blue line) and shows that alternations in horizontal motion rivalry have a single peak at the rotation frequency (0.25 Hz). In contrast, perceptual alternations for motion rivalry in the stationary control (yellow line) reveals only low-amplitude peaks at several points scattered over the frequency range.

Figure 2C shows the pattern in 2b was consistent over observers (thin blue lines), with rivalry alternation rates for 11/14 subjects peaking very near the 0.25 Hz rotation frequency. The group mean peaked at 0.24 Hz (95% CI = [0.220, 0.259]; two-tailed t test against 0.25 Hz: $t(13) = -1.21$, $p = .2486$). When the same observers viewed horizontal motion rivalry while stationary (thin yellow lines), the frequency peaks were scattered, low amplitude and variable among observers (see yellow arrows, and box-and-whisker plot). Similarly, when viewing vertical motion rivalry (Figure 2D), there were no systematic peaks at the (horizontal) rotation frequency. These results show, first, that the effect depends on rotation and is thus vestibular in origin, and second, that it is a tuned visual-vestibular interaction that requires congruent motion/rotation trajectories.

The absence of a dominant perceptual oscillation frequency for the pairing of vertical motion rivalry with horizontal rotation rules out the possibility that the strongly cyclic rivalry time course seen in Figure 1C for yaw rotation with horizontal motion rivalry arose from a response bias where observers changed response buttons with each reversal of rotation direction. It also shows that perceptual switches were not driven by transient neural responses (which can provoke rivalry switches (Walker, 1975)) arising when the rotation direction is reversed.

Figure 2E shows rivalry alternation data for horizontal motion rivalry aggregated over all observers, contrasting the stationary and yaw rotation conditions. To obtain these plots, the rivalry time course data have been divided into 4-s periods and then combined into a single cycle. In doing so, we make the strong assumption that a 0.25 Hz yaw rotation will entrain a rivalry oscillation at 0.25 Hz and see how well the data and prediction match. The data are shown at the tracking resolution of 60 Hz without any binning or
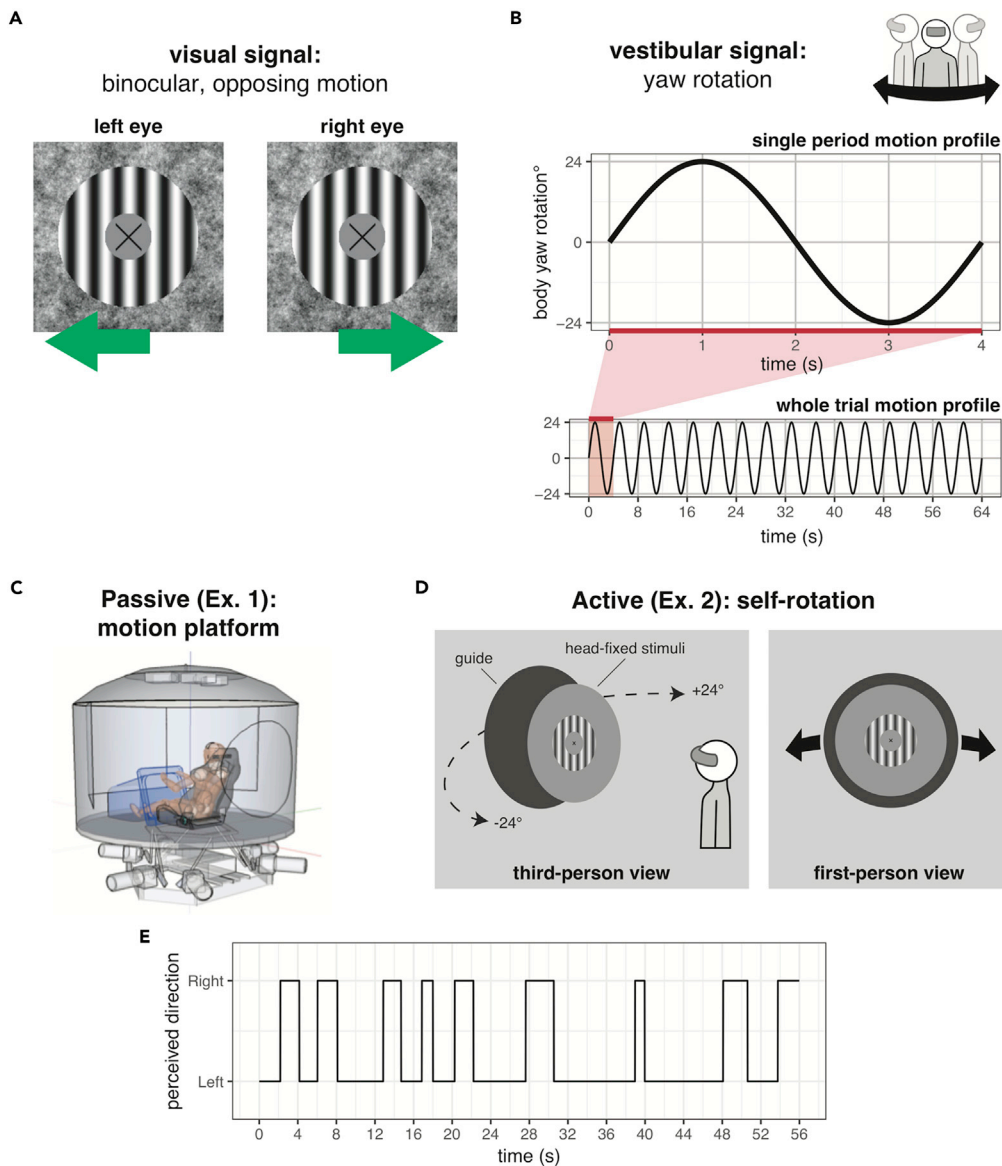
Figure 1. Stimuli and methods

(A) Binocular rivalry stimuli were sinusoidal gratings drifting in opposite directions, either horizontally or vertically. The gratings drifted within centrally located apertures that remained stationary in head-defined coordinates during rotation. A central gray disk and fixation cross were used to stabilize fixation and prevent following eye movements (see Figure S1) so that the only visual motion came from the opposed gratings which drifted with a constant retinal velocity in central vision.

(B) Yaw rotation was sinusoidal with an amplitude of $\pm24°$ and full cycle period of 4 s (0.25 Hz). Single trials involved 16 cycles of rotation (64 s), repeated eight times per condition.

(C) Passive yaw rotation: Observers sat on a motion platform and viewed the vertical or horizontal rivalry stimuli through a head-mounted display.

(D) Active yaw rotation: Observers were seated on a stool and rotated their head while viewing the rivalry stimuli in the head-mounted display, following a dark circular guide which surrounded the grating stimuli and oscillated in real-world coordinates through $\pm24°$ at 0.25 Hz (for simplicity, only one grating is shown). By keeping the gratings centered within the surrounding guide (see first-person view in Video S1), the active and passive rotations were matched. Head tracking confirmed subjects accurately followed the guide (see Figures 3E and 3F).

(E) The task was to continuously track the perceptual alternations of the rivaling visual motions and participants were told that rotation was task-irrelevant. The plot shows one trial of tracking data for a single observer and illustrates that binocular rivalry alternations (typically highly irregular) become unusually cyclic during yaw rotation.
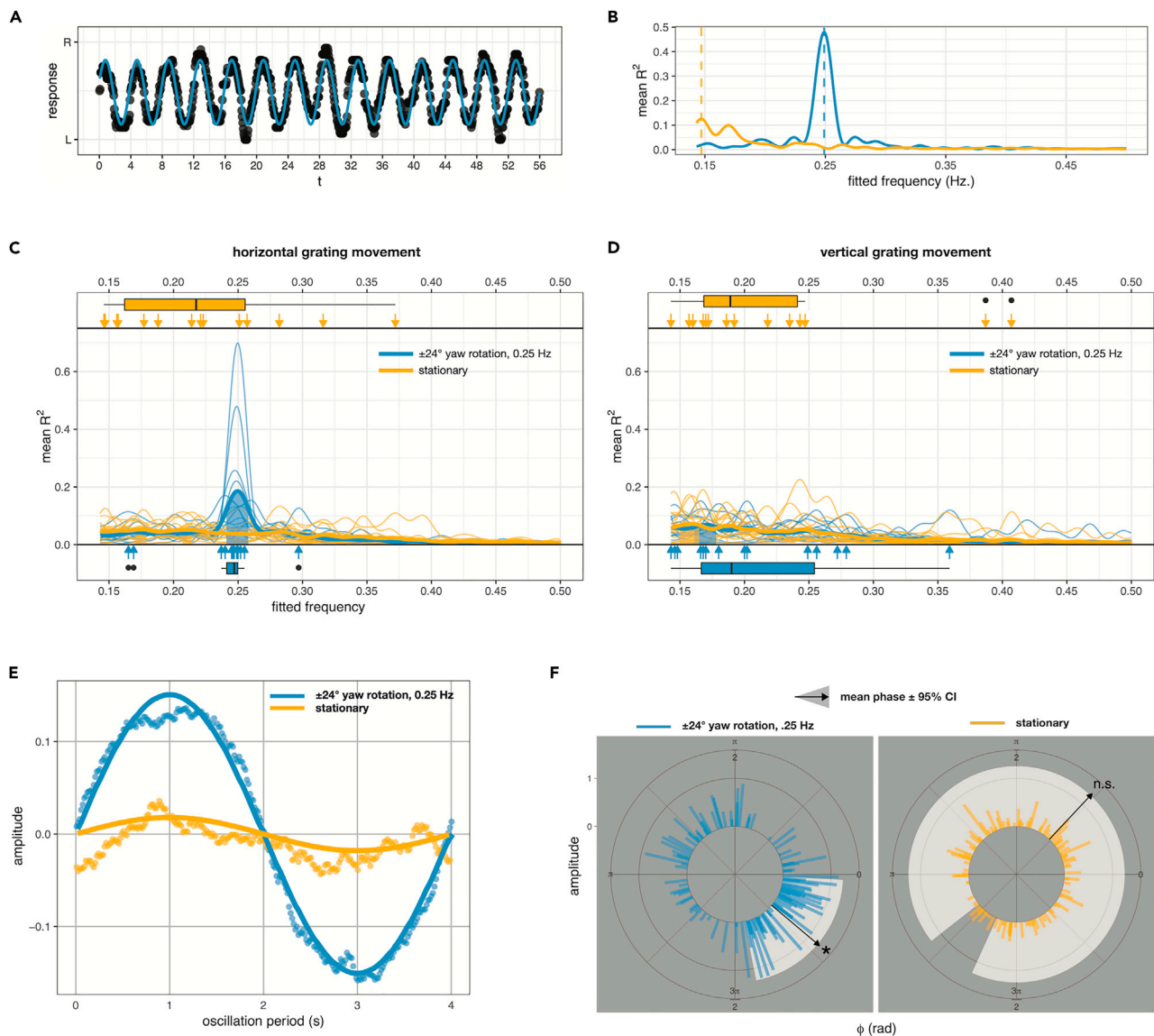
Figure 2. Results from Experiment 1: passive yaw rotation at 0.25 Hz

(A) One participant's data showing the mean of eight trials of continuously tracking perceived visual direction for horizontal motion rivalry during yaw rotation. Blue line: best fitting sinusoid.

(B) Goodness-of-fit for a broad range of sinusoids fitted to this participant's data shows a typical pattern: a prominent, single peak in rivalry alternations near 0.25 Hz for rotation (blue) but not stationary (yellow).

(C) Results for all observers (n = 14) for horizontal motion rivalry during passive rotation (blue) and stationary control (yellow). During rotation, perceptual alternations show a peak frequency close to rotation rate; when stationary, alternation rates were weak and widely distributed. Arrows show the frequency of each participant's best-fitting sinusoid.

(D) For vertical motion rivalry, perceptual alternations showed no clear periodicity for rotation or stationary.

(E) A 0.25-Hz sinusoid was fitted to the alternation data after it was aggregated over all observers and trials and binned into 4-s periods. The data for rivaling horizontal motions conform very well to a 4-s sinusoid. Note that raw data were used for fitting (no averaging or smoothing) although the data points added for illustration show the aggregate data averaged into 60 Hz bins.

(F) Phase and amplitude of a 0.25-Hz sinusoid fitted to every trial's perceptual alternation data for horizontal motion rivalry during rotation (left, blue) and while stationary (right, yellow). The arrow and shading show mean phase and 95% confidence interval.

smoothing and each data symbol shows the mean of the overlaid cycles at a given sample point. The continuous line is the best-fitting sinusoid fixed at 0.25 Hz (amplitude and phase were free to vary) and clearly shows an excellent match between the rivalry alternation data and the 0.25 Hz yaw rotation. The amplitude for the yaw rotation condition is 0.151 (95% CI = [0.147, 0.154]), significantly higher than for

stationary (amplitude = 0.018; 95% CI = [0.013, 0.022]). The very close match between the rotation frequency and the alternation of perceived visual motion during rivalry is consistent with a single oscillatory driver operating at 0.25 Hz causing the perceptual alternations.

Because the rivalry data conformed so well to a 0.25 Hz oscillation, we were able to analyze the phase of perceptual alternations relative to rotation by fitting each participant's alternation time course with a fixed 0.25-Hz sinusoid (with phase and amplitude free). The best-fitting phase and amplitude for horizontal motion rivalry are plotted in Figure 2F for rotation (left, blue) and stationary (right, yellow). Both show 112 vectors (14 participants × 8 trials) representing phase and amplitude of every trial, with group mean (dark arrow) and 95% confidence interval. Amplitudes for the stationary condition were small (mean = 0.105) and phases were widely scattered and did not pass the Rayleigh test for non-uniformity (z = 0.547, p = 0.580). Amplitudes were greater for rotation (mean = 0.279) and phase angles were clustered (Rayleigh test: z = 8.736, p < .0005) with a mean of 328.66° and narrow confidence interval. Given a 4-s cycle, the mean phase corresponds to perceptual alternations lagging rotation by roughly half a second (see also Figure 4): a lagged but positively correlated response (leftward motion is seen during leftward rotation, rightward during rightward rotation). There was no phase clustering for yaw rotation if the rivaling motions were vertical (mean amplitude 0.063, Rayleigh test: z = 0.315, p = .731), showing a direction-selective effect requiring congruent trajectories.

Experiment 2: active self-rotation

The first experiment isolated a vestibular effect on visual motion rivalry using passive rotation. Experiment 2 repeats the same conditions and analyses with active yaw rotation. The observer's task was to turn their head while seated on a stool to follow a visual guide presented in the head-mounted display which oscillated – in real-world coordinates – with the same amplitude and rate as Experiment 1 (±24°, 0.25 Hz). A video of the task illustrated in Figure 1D, taken from first-person perspective, is available as Video S1. Observers were instructed to rotate in a manner that was comfortable and repeatable using a combination of head and body rotation. Figures 3E and 3F confirm that the observers were able to follow the guide consistently and accurately.

When motion rivalry was horizontal (Figure 3A), observers' rivalry time-courses in the yaw rotation condition (blue lines) had best-fitting sinusoids tightly clustered near the rotation frequency (mean = 0.25 Hz, 95% CI = [0.249, 0. 255], two-tailed t test against 0.25 Hz: t(9) = 1.42, p = .1894). Viewing the same rivaling motions when stationary showed neither systematic peak nor high variability across the group (yellow lines). Vertical motion rivalry (Figure 3B) also produced low amplitude and high variability, for active rotation (blue lines) and stationary (yellow lines). Although there does appear to be a small cluster at the rotation frequency for vertical rivalry with active yaw rotation (Figure 3B), the group mean rivalry alternation rate is significantly different from the rotation rate (two-tailed t test against 0.25 Hz: t(9) = −2.26, p = .04994). Moreover, participants varied considerably in their rivalry alternation rate in this condition (compare blue arrows in Figures 3B vs. 3A). The apparent peak at 0.25 Hz is driven mainly by one participant who has a clear peak at ∼0.25 Hz. A second participant shows a local peak at ∼0.25 Hz, but it is much lower in amplitude than the outlier participant and it is in fact a secondary peak for that observer. Overall, as for passive rotation, active yaw rotation strongly entrained rivalry alternations to the rotation frequency in a direction-selective way: only horizontal motion rivalry produced the effect.

To reveal the amplitude of the entrainment of rivalry alternations to the rotation cycle and verify the sinusoidal pattern of the rivalry time course, we aggregated the data in the horizontal rivalry condition and combined it into a single 4-s cycle. In Figure 3C, the best-fitting 0.25 Hz sinusoid (with amplitude and phase free) is overlaid on the single-cycle rivalry data (amplitude = 0.237; 95% CI = [0.233, 0.242]) and shows an excellent match with the data, consistent with perceptual alternations being driven by a single oscillatory driver at 0.25 Hz. The amplitude in the stationary conditions was low (0.024, 95% CI = [0.020, 0.029]) and the data was complex and inconsistent with a single frequency component.

With the rivalry alternation data conforming so well to a 0.25 Hz oscillation, we conducted an analysis of phase at that frequency by fitting every trial with a fixed 0.25-Hz sinusoid (with phase and amplitude free). Figure 3D shows phases for horizontal motion rivalry in rotation (left, blue) and stationary (right, yellow). Each plot has 80 radial lines (10 participants × 8 trials) showing phase and amplitude of the best-fitting 0.25-Hz sinusoid, with mean phase (arrow) and 95% confidence interval. Amplitudes for stationary were
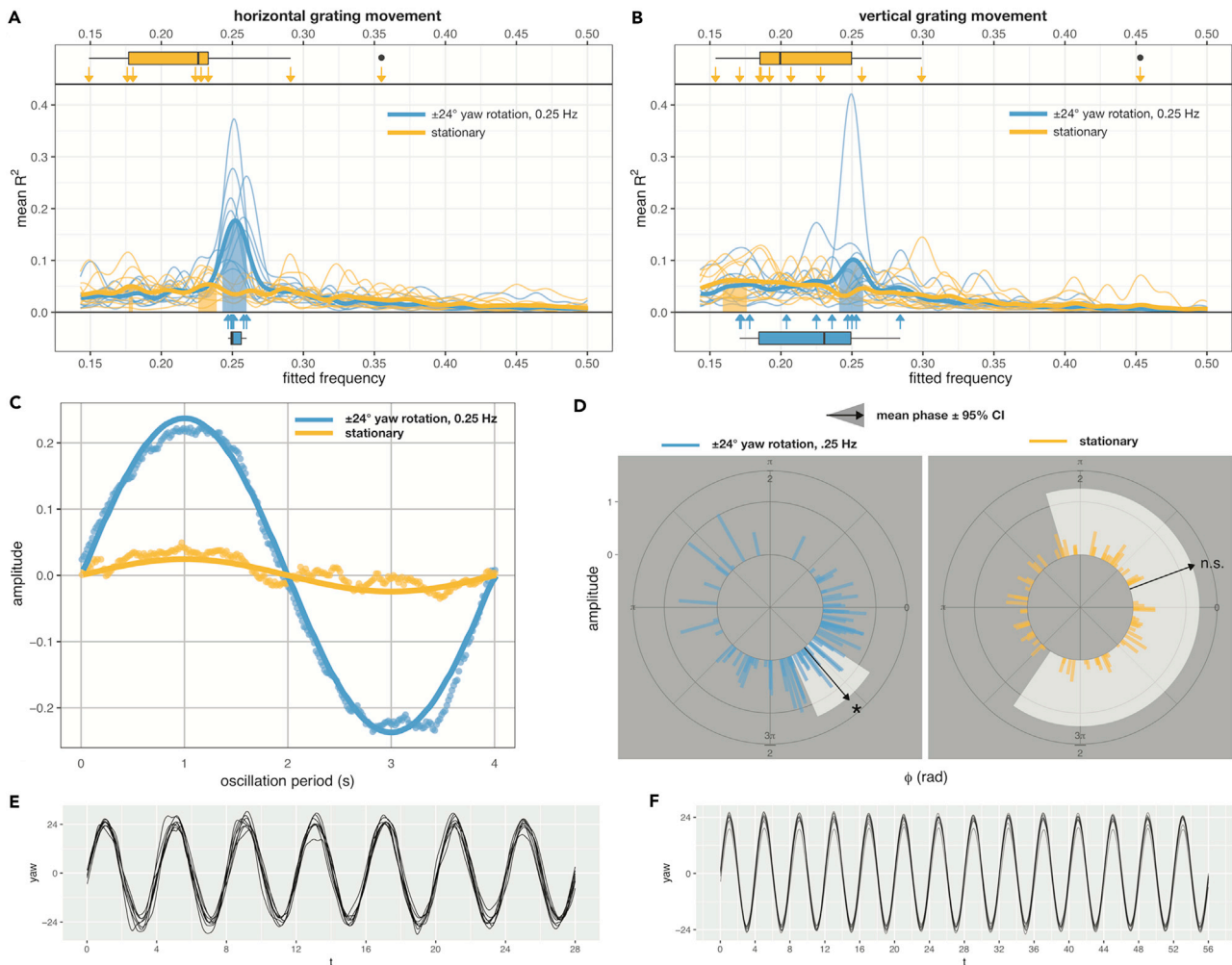
Figure 3. Results from Experiment 2: active yaw rotation at 0.25 Hz. Formats and conventions as in Figure 2

(A) Group results (n = 10) for horizontal motion rivalry during active yaw rotation (blue) and stationary control (yellow). Rivalry alternations in active rotation closely matched the rotation frequency, while alternation rates for stationary were widely distributed.

(B) Vertical motion rivalry for active rotation (blue) and stationary (yellow) both showed distributed alternation rates.

(C) Aggregated alternation data for all trials, binned into 4-s periods and pooled, for rivaling horizontal motions.

(D) Phase and amplitude of a 0.25-Hz sinusoid fitted to every trial's perceptual alternation data for horizontal motion rivalry during rotation (left, blue) and stationary (right, yellow). The arrow and shading show mean phase and 95% confidence interval.

(E) One observer's head position over time for 8 trials of active rotation. The trials overlay each other very consistently (for better resolution, only the first half of each trial is shown).

(F) Head-tracking data for all participants showing, each an average of both rotation conditions (16 trials). Observers accurately approximated a 4-s period and ±24° amplitude.

small (mean = 0.162) and phases were widely scattered and did not pass the Rayleigh test for non-uniformity (z = 2.105, p = .122). Amplitudes were greater for rotation (mean = 0. 522) and phase angles were clustered (Rayleigh test: z = 21.760, p < .0001) with a mean of 313.76° and narrow confidence interval. The mean phase corresponds to perceptual alternations lagging the rotation cycle by slightly less than half a second and thus positively correlated with rotation direction, as found for passive rotation.

Comparison of passive versus active rotation effects

Active and passive yaw rotation were both effective at entraining the time course of horizontal motion rivalry to the rotation cycle of 0.25 Hz (see Figures 2C and 3A). However, entrainment to the rotation frequency was more consistent across observers in active self-rotation. As shown by the arrows in Figure 3A representing each participant, there was almost no variation among observers in the alternation rate of the
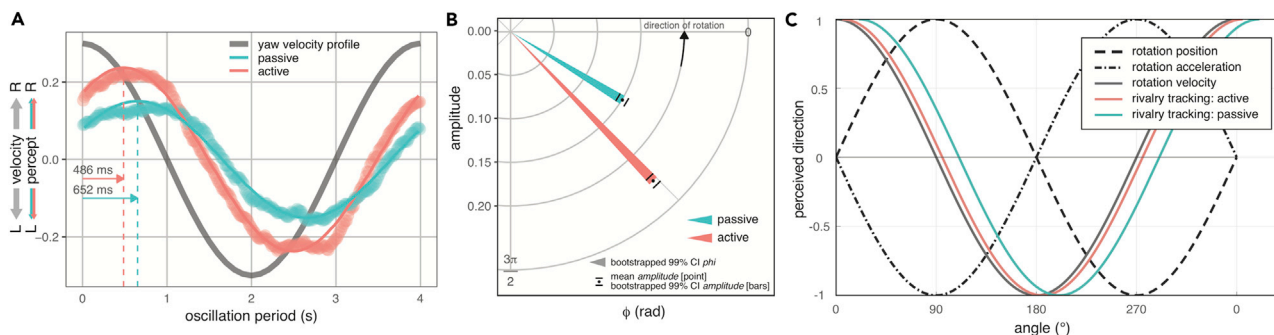
Figure 4. Entrainment of perceived direction by active and passive rotation during horizontal motion rivalry

(A) Aggregated data for active and passive rotation compiled into a single cycle and overlaid with the best-fitting 4-s sinusoid. The sinusoids are offset by their respective phase lags relative to rotation velocity, with the lag for active rotation (red) shorter than passive (green) by 166 ms.

(B) Polar plot of the data in panel (A) The shaded wedges show 99% confidence intervals around phase angle and their lengths show group mean amplitude with 99% confidence intervals.

(C) The best-fitting sinusoids from panel a are plotted after a component for decision and response time (several hundred milliseconds: see main text) has been subtracted, shifting the plots leftward. The dashed lines plot rotation in terms of position and acceleration (±90° phase shifts of velocity). With response time subtracted, perceived visual direction exhibits a tight positive correlation rotation velocity (bold line) and is independent of position or velocity.

rivalry time course and it matched very closely the 0.25 Hz rotation cycle. For passive rotation, entrainment to the rotation cycle was still impressively consistent and close to the rotation rate (Figure 2C); however, two of 14 observers lie away from the group mean and the main cluster is more variable than for active rotation.

The strength of entrainment of rivalry alternations to the rotation cycle was stronger in the active rotation condition, as seen by comparing the amplitude of the single-cycle plots (Figure 2E vs. 3C). The phase analyses also confirm a stronger entrainment effect for active rotation, with the mean resultant magnitude for active rotation (0.522) being significantly greater than for passive rotation (0.279) on a bootstrap sign test (p = .0001; 10,000 iterations). The phase of rivalry's entrainment to the rotation cycle also differed between active and passive (Figures 4A and 4B). Using a bootstrap sign test, we resampled the group mean rivalry time course for active and passive 10,000 times, fitting a 0.25-Hz sinusoid on each iteration (with phase and amplitude free) and compared the phase of entrainment in the active and passive conditions. Phase for active rotation was reliably earlier than for passive (p = .0002). The mean difference was 14.94°, a time difference of 166 ms for a 4-s cycle, meaning rivalry alternations in perceived direction for the active condition entrained to the rotation cycle with a shorter time-lag than for passive rotation.

Figure 4A summarizes the amplitude and phase differences in rivalry entrainment between active and passive rotation conditions. It differs from Figures 2E and 3C by showing the best-fitting 0.25-Hz sinusoids with phase offsets included (active more leftward than passive by 166 ms), and by plotting rotation as velocity instead of position over time (thus giving it a cosine phase). The amplitude and phase parameters are also compared in the polar plot in Figure 4B, plotted with 99% confidence intervals. An important component of phase offset will be the participant's decision and response time. From a previous study using unsped tracking of extended rivalry trials, this value is about 425 ms (Alais et al., 2010). Subtracting this value from the phase lags in Figure 4A reveals a strong positive correlation between rotation velocity and perceived visual direction (Figure 4C): as rightward velocity rises, so does the likelihood of perceiving rightward visual motion (and *vice versa*). The dashed lines in Figure 4C also show rotation plotted in terms of position and acceleration (sinusoids shifted ±90° from the velocity plot), revealing the perceptual data are effectively independent of rotation position and rotation velocity.

DISCUSSION

The present study reports a striking influence of both vestibular and action signals in resolving ambiguous visual input. By presenting opposed visual motions, one to each eye, an ongoing stochastic switching of motion directions is perceived as each eye is alternately suppressed, whereas the other temporarily dominates. Using passive whole-body rotation in the yaw (horizontal) plane, Experiment 1

demonstrated that vestibular signals entrained the erratic alternations of perceived visual direction into a cyclic pattern matching the rotation frequency (0.25 Hz) and positively correlated with it: leftward visual motion perceived duration leftward rotation, and rightward motion during rightward rotation. Yaw rotation did not entrain rivalry between opposed vertical motions (i.e., orthogonal to rotation plane) or during no-rotation trials, confirming the effect is a directionally-selective visual-vestibular interaction. Repeating these conditions in Experiment 2 using self-rotation showed that active movement produced the same pattern of results as passive, although the effect was stronger for active rotation and perceptual alternations, followed by the rotation cycle with a shorter time lag. As in Experiment 1, the vertical motion rivalry condition served as a control to check that participants did not simply exhibit a bias in which their motion-tracking responses were driven by reversals in rotation direction. In Experiment 2 it is clear that one subject in this condition responded consistently with a response bias (none in Experiment 1) and showed a peak at the rotation frequency when it is not expected. For nine of the ten subjects, however, the vertical rivalry data are very similar in the motion and static conditions, arguing against a simple response bias linked to rotation reversals and thus imply a directionally selective coupling of rotation and motion rivalry. Future experiments could investigate this further by using a rivalry replay condition based on the static rivalry condition and presenting it during rotation to see whether rivalry tracking would follow the replay or the rotation cycle.

The entrainment of horizontal motion rivalry to the yaw rotation rate is unusual in that it violates two well-known characteristics of binocular rivalry dynamics. First, perceptual alternation rate in binocular rivalry varies markedly between individuals (Carter and Pettigrew, 2003; Gallagher and Arnold, 2014), yet rotation caused all participants to alternate at the rotation rate of 0.25 Hz. Second, sequences of dominance durations are largely serially independent and thus follow stochastic patterns over time (Fox and Herrmann, 1967; van Ee, 2009; Walker, 1975), yet rotation causes rivalry to alternate cyclically. When the observer was stationary or viewed vertical motion rivalry while rotating, both these characteristics were present: Individual differences in alternation rate are obvious in the large range of means in Figures 2C and 3A (see arrows), and the irregularity of perceptual alternations is evident in the broad frequency spectra in Figures 2C, 2D, 3A, and 3B. In contrast, both these fundamental characteristics of rivalry were violated in the congruent visual/rotation condition or else cyclic alternations at the rotation frequency could not have occurred. The data confirm this: mean alternation rates agreed closely among observers at 0.25 Hz and rivalry alternations were cyclically entrained, showing a prominent narrow peak in the frequency spectra (Figures 2C and 3A; lower box plotand-whisker plot). Notably, rotation altered observers' baseline alternation rates in two ways: slow switchers (oscillation periods >4 s) sped up, meaning long dominance periods were curtailed by rotation reversals, whereas fast switchers slowed down so that perceptual changes were delayed to align with rotation reversals.

What might cause rivalry alternation rates to shift into alignment with the rotation rate? We suggest the visual and rotation signals are combined and alter the relative strength between the two competing visual signals. This squares with recent multisensory studies of binocular rivalry (Conrad et al., 2010; Hense et al., 2019; Lunghi et al., 2014) showing that congruent crossmodal stimuli modulate binocular rivalry alternations. These crossmodal influences can be tightly tuned for feature congruence (Lunghi and Alais, 2013; Lunghi et al., 2014) and can modulate rivalry by both extending rivalry phases when the crossmodal stimulus is congruent with dominant visual stimulus and shortening rivalry phases when it is not, thereby hastening the re-emergence of the suppressed (but congruent) image (Lunghi and Alais, 2015). With vestibular rotation signals projecting into visual motion area MST (Gu et al., 2008; Takahashi et al., 2007), the changing sign of rotation could directly modulate the competing visual motion signals – either in MST or by feedback projections to MT or even V1. Thus vestibular input to the visual competition process underlying binocular rivalry could explain the results in an analogous way to earlier results (Lunghi and Alais, 2013, 2015).

Mutual inhibition models of rivalry propose that rivalry dominance changes occur when neurons representing the visible stimulus begin to adapt, releasing the competing neural pool from inhibition until their response levels crossover and a perceptual switch occurs (Alais et al., 2010). If rotation signals were combined with visual motion signals, whether in MST or fed back to earlier levels, they would strengthen and help maintain dominance of the congruent visual motion for longer, thereby explaining why fast-switching participants slowed down their rivalry rate. Conversely, for slow switchers, a reversal of rotation direction would abruptly boost the suppressed direction and promote it into dominance, thereby speeding up their switch rate. The rate of rotation may be critical here, too. Although 0.25 Hz was chosen because it was the maximum rate available on the motion platform, it was serendipitous as rotation direction reversed every

2 s, similar to typical rivalry dominance durations. This meant that each change in rotation direction occurred when the rivalry alternation process was close to switching and could be most effectively biased by a crossmodal stimulus, either extending the current dominance phase or curtailing it when a rotation reversal then favored the opposite visual motion.

Figure 4A shows the data for perceived visual direction correlate very well with rotation velocity. The peak likelihood of a rightward percept follows shortly after peak rightward rotation velocity, and *vice versa*. The correlation between perception and rotation velocity is even stronger than suggested in the figure because part of the lag in the perceptual data is due to the observer's decision and response time. Figure 4C shows yaw rotation plotted as a function of position, velocity and acceleration, with single cycles of the perceptual data overlaid. In an earlier study that also involved extended trials of (unspeeded) rivalry tracking (Alais et al., 2010), we estimated decision/response time to be about 425 ms. Subtracting this amount from the data shifts the perceptual cycles to a near-perfect alignment with the velocity function, and thus orthogonal to the position and acceleration functions. The close alignment between the perceptual data and the velocity function highlights the positive correlation between the two: leftward motion was perceived during leftward rotation, and rightward motion during rightward rotation.

What explains the strong association between rotation and perceived visual direction? The well-known predictive or 'forward' models (Wolpert and Flanagan, 2001) of motor control used to explain the sensory consequences of action provide an account of the active condition. The key element of forward models is that efference copy of motor commands is used to model the sensory activity that will arise from a voluntary action. This sensory prediction can be used to attenuate (Blakemore et al., 1999) or even completely cancel (Cullen, 2019) the sensory effects of the voluntary movement (i.e., reafference) so that it is not confounded with externally generated sensory responses (exafference). Studies comparing vestibular activity during active and passive head movements show that the response due to voluntary head movement is completely subtracted from vestibular activity (Cullen, 2012). Attenuation of reafferent visual signals also occurs following voluntary action, as demonstrated in behavioral and neural studies (Benazet, et al., 2016; Mifsud, et al., 2018; Stenner, et al., 2014). In our active rotation condition, the reafference expected while making a head turn to the left, for example, is visual motion to the right. Attenuating the 'reafferent' rightward motion would then leave the leftward visual motion as the dominant sensory signal. In binocular rivalry, perception is generally determined by the strongest or most salient stimulus (Alais, 2012), and thus this attenuation account would explain the positive correlation between head-turn direction and perceived visual direction in the active condition.

Explaining the positive relationship between rotation and visual direction during passive rotation is less clear, although we propose an analogous account based on visual-vestibular neurophysiology. Visual-vestibular neurons are found in several cortical areas, MSTd, VIP, and FEF (Bremmer et al., 2002; Gu et al., 2006, 2016; Takahashi et al., 2007), and are classified into two types based on their directional selectivity. 'Congruent' cells respond to head and visual motion in the same direction, whereas 'opposite' cells respond preferentially to opposed head and visual motions. For translational movement, both types are found in similar proportions in all visual-vestibular areas. For rotational movement, in contrast, only oppositely tuned visual-vestibular cells are found (Takahashi, et al., 2007). These prefer head rotation and visual motion in opposite directions. It is still unknown why they only occur in the 'opposite' configuration (Zhang, et al., 2019); however, opposite-tuned rotation cells may be used to compensate for the confounding effects of rotatory head movements on optic flow (Takahashi, et al., 2007). In other words, a passive head rotation in a given direction is linked with a visual 'counter-rotation' to be subtracted from retinal input to preserve optic flow. Oppositely tuned rotation neurons would therefore play the same canceling role in a passive context as the predicted sensory response does in an active, forward-model context, thereby explaining the positive rotation/visual direction correlation for passive rotation.

A final intriguing point is that the perceptual data exhibits a shorter phase lag for active rotation compared to passive (Figure 4). One key difference between active and passive movements is an earlier sensory response for active movement. This is seen in faster active responses for limb and head movements (London and Miller, 2013; van der Meer et al., 2007) by about 100 ms and in head-direction cells (Taube, 2007) which respond faster to active rotations (Zugaro et al., 2001) to anticipate head position by nearly 100 ms (van der Meer et al., 2007). This is understood in terms of 'forward models' where motor efference copy sent to sensory circuits generates an expected response that anticipates the slower arriving sensory afferents

(Roy and Cullen, 2001; Sommer and Wurtz, 2008). This faster active response is similar in magnitude to the phase advance we report for active relative to passive (166 ms).

In sum, viewing binocular rivalry between horizontally opposed visual motions while undergoing yaw rotation causes suppression of the visual direction opposed to rotation so that visual perception is resolved to match rotation. Similar data patterns are obtained for active and passive rotations and we propose that both can be explained by different but functionally similar processes which attenuate expected visual activity arising from rotation. For active rotation, a forward model of sensorimotor action could achieve this discounting of reafference, whereas for passive rotation we conjecture that a functionally similar process predicts expected visual activity using oppositely tuned visual-vestibular rotation cells. In both cases, attenuating the opposite direction leaves the congruent visual direction perceptually dominant, with the shorter phase lag for active rotation because of the predictive nature of forward modeling, whereas the passive condition is reactive in relying on a vestibular signal that rotation has occurred. Future studies examining how binocular rivalry between various visual motions is resolved by rotations or translations could provide further insights into visual-vestibular interaction and the proposed reafferent attenuation account.

Limitations of the study

Our study focused on sinusoidal rotations, which was largely due to equipment constraints. Although this was clearly sufficient to demonstrate a strong crossmodal interaction between self-rotation and ambiguous visual direction, it would be of interest to see whether a less predictable motion would also show a similar effect. This would help test whether top-down influences such as expectation of rotation reversals contributed to the effects we report. Less predictable motions would inevitably contain more fluctuations in velocity, leading also to the question of what exactly is the ideal relationship between rotation velocity and visual stimulus velocity and how tightly it is tuned for relative velocity.

This study also used visual gratings that drifted with constant velocity while the rotation velocity was sinusoidal. Our lab will soon have the capacity to produce continuous rotations, which will allow us to examine constant grating and rotation velocities to better explore their velocity dependency. The current study is unable to conclude whether the correlation between perceived visual direction and rotation direction was simply because of directional correspondence and thus should be maintained in a regime of continuous rotation. Another consideration is whether the clear entrainment we report here was partly because of the sinusoidal reversals having a similar period to typical rivalry reversal rates. Future studies could easily explore this further by varying the period of sinusoidal rotation and/or the speed of the visual stimuli. Even if there is a link between the rotation period and rivalry period, it still leaves the two key findings reported here intact, namely, (i) that self-rotation and visual direction ambiguity show a strong crossmodal interaction, and (ii) that this crossmodal relationship is a positive one in which perceived visual direction correlates with rotation direction.

STAR★METHODS

Detailed methods are provided in the online version of this paper and include the following:

- KEY RESOURCES TABLE
- RESOURCE AVAILABILITY
  - Lead contact
  - Materials availability
  - Data and code availability
- EXPERIMENTAL MODEL AND SUBJECT DETAILS
  - Participants
- METHOD DETAILS
  - Apparatus
  - Stimuli
  - Procedure
- QUANTIFICATION AND STATISTICAL ANALYSIS

SUPPLEMENTAL INFORMATION

Supplemental information can be found online at https://doi.org/10.1016/j.isci.2021.103417.

REFERENCES

Alais, D. (2012). Binocular rivalry: competition and inhibition in visual perception. Wiley Interdiscip. Rev. Cogn. Sci. *3*, 87–103.

Alais, D., and Blake, R. (2005). Binocular Rivalry (Cambridge: MA: MIT Press).

Alais, D., and Blake, R. (2015). Binocular rivalry and perceptual ambiguity. In The Oxford Handbook of Perceptual Organization, J. Wagemans, ed. (Oxford University Press).

Alais, D., Cass, J., O'Shea, R.P., and Blake, R. (2010). Visual sensitivity underlying changes in visual consciousness. Curr. Biol. *20*, 1362–1367.

Benazet, M., Thenault, F., Whittingstall, K., and Bernier, P.M. (2016). Attenuation of visual reafferent signals in the parietal cortex during voluntary movement. J. Neurophysiol. *116*, 1831–1839.

Benson, A.J., and Brown, S.F. (1989). Visual display lowers detection threshold of angular, but not linear, whole-body motion stimuli. Aviat. Space Environ. Med. *60*, 629–633.

Blake, R., and Logothetis, N.K. (2002). Visual competition. Nat. Rev. Neurosci. *3*, 13–21.

Blake, R.R., Fox, R., and McIntyre, C. (1971). Stochastic properties of stabilized-image binocular rivalry alternations. J. Exp. Psychol. *88*, 327–332.

Blakemore, S.J., Frith, C.D., and Wolpert, D.M. (1999). Perceptual modulation of self-produced stimuli: the role of spatio-temporal prediction. J. Cogn. Neurosci. *11*, 551–559.

Bremmer, F., Klam, F., Duhamel, J.R., Ben Hamed, S., and Graf, W. (2002). Visual-vestibular interactive responses in the macaque ventral intraparietal area (VIP). Eur. J. Neurosci. *16*, 1569–1586.

Carter, O.L., and Pettigrew, J.D. (2003). A common oscillator for perceptual rivalries? Perception *32*, 295–305.

Chen, A., Deangelis, G.C., and Angelaki, D.E. (2013). Functional specializations of the ventral intraparietal area for multisensory heading discrimination. J. Neurosci. *33*, 3567–3581.

Conrad, V., Bartels, A., Kleiner, M., and Noppeney, U. (2010). Audiovisual interactions in binocular rivalry. J. Vis. *10*, 27.

Cullen, K.E. (2012). The vestibular system: multimodal integration and encoding of self-motion for motor control. Trends Neurosci. *35*, 185–196.

Cullen, K.E. (2019). Vestibular processing during natural self-motion: implications for perception and action. Nat. Rev. Neurosci. *20*, 346–363.

Dichgans, J., and Brandt, T. (1978). Visual-vestibular interaction: effects on self-motion perception and postural control. In Handbook of Sensory Physiology, R. Held, H. Leibowitz, and H.-L. Teuber, eds. (Springer), pp. 755–804.

Duffy, C.J. (1998). MST neurons respond to optic flow and translational movement. J. Neurophysiol. *80*, 1816–1827.

Fox, R., and Herrmann, J. (1967). Stochastic properties of binocular rivalry alternations. Percept. Psycho. *2*, 432–436.

Gallagher, R.M., and Arnold, D.H. (2014). Interpreting the temporal dynamics of perceptual rivalries. Perception *43*, 1239–1248.

Gu, Y., Angelaki, D.E., and Deangelis, G.C. (2008). Neural correlates of multisensory cue integration in macaque MSTd. Nat. Neurosci. *11*, 1201–1210.

Gu, Y., Watkins, P.V., Angelaki, D.E., and DeAngelis, G.C. (2006). Visual and nonvisual contributions to three-dimensional heading selectivity in the medial superior temporal area. J. Neurosci. *26*, 73–85.

Gu, Y., Cheng, Z., Yang, L., DeAngelis, G.C., and Angelaki, D.E. (2016). Multisensory convergence of visual and vestibular heading cues in the pursuit area of the frontal eye field. Cereb. Cortex. *26*, 3785–3801.

Hense, M., Badde, S., and Roder, B. (2019). Tactile motion biases visual motion perception in binocular rivalry. Atten. Percept. Psycho. *81*, 1715–1724.

London, B.M., and Miller, L.E. (2013). Responses of somatosensory area 2 neurons to actively and passively generated limb movements. J. Neurophysiol. *109*, 1505–1513.

Lopez, C., and Blanke, O. (2011). The thalamocortical vestibular system in animals and humans. Brain Res. Rev. *67*, 119–146.

Lunghi, C., and Alais, D. (2013). Touch interacts with vision during binocular rivalry with a tight orientation tuning. PLoS One *8*, e58754.

Lunghi, C., and Alais, D. (2015). Congruent tactile stimulation reduces the strength of visual suppression during binocular rivalry. Sci. Rep. *5*, 9413.

Lunghi, C., Morrone, M.C., and Alais, D. (2014). Auditory and tactile signals combine to influence vision during binocular rivalry. J. Neurosci. *34*, 784–792.

Lyons, R.G. (2011). Understanding Digital Signal Processing, *Thrid edition* (Prentice-Hall).

Mifsud, N.G., Beesley, T., Watson, T.L., Elijah, R.B., Sharp, T.S., and Whitford, T.J. (2018). Attenuation of visual evoked responses to hand and saccade-initiated flashes. Cognition *179*, 14–22.

Roy, J.E., and Cullen, K.E. (2001). Selective processing of vestibular reafference during self-generated head motion. J. Neurosci. *21*, 2131–2142.

Schlack, A., Hoffmann, K.P., and Bremmer, F. (2002). Interaction of linear vestibular and visual stimulation in the macaque ventral intraparietal area (VIP). Eur. J. Neurosci. *16*, 1877–1886.

Sommer, M.A., and Wurtz, R.H. (2008). Brain circuits for the internal monitoring of movements. Annu. Rev. Neurosci. *31*, 317–338.

Stenner, M.P., Bauer, M., Haggard, P., Heinze, H.J., and Dolan, R. (2014). Enhanced alpha oscillations in visual cortex during anticipation of self-generated visual stimulation. J. Cogn. Neurosci. *26*, 2540–2551.

Takahashi, K., Gu, Y., May, P.J., Newlands, S.D., DeAngelis, G.C., and Angelaki, D.E. (2007). Multimodal coding of three-dimensional rotation and translation in area MSTd: comparison of visual and vestibular selectivity. J. Neurosci. *27*, 9742–9756.

Taube, J.S. (2007). The head direction signal: origins and sensory-motor integration. Annu. Rev. Neurosci. *30*, 181–207.

van der Meer, M.A., Knierim, J.J., Yoganarasimha, D., Wood, E.R., and van Rossum, M.C. (2007). Anticipation in the rodent head direction system can be explained by an interaction of head movements and vestibular firing properties. J. Neurophysiol. *98*, 1883–1897.

van Ee, R. (2009). Stochastic variations in sensory awareness are driven by noisy neuronal adaptation: evidence from serial correlations in perceptual bistability. J. Opt. Soc. Am. A Opt. Image Sci. Vis. *26*, 2612–2622.

Walker, P. (1975). Stochastic properties of binocular rivalry alternations. Percept. Psycho. *18*, 467–473.

Wolpert, D.M., and Flanagan, J.R. (2001). Motor prediction. Curr. Biol. *11*, R729–R732.

Zhang, W.H., Wang, H., Chen, A., Gu, Y., Lee, T.S., Wong, K.Y.M., and Wu, S. (2019). Complementary congruent and opposite neurons achieve concurrent multisensory integration and segregation. eLife *8*, e43753.

Zugaro, M.B., Tabuchi, E., Fouquier, C., Berthoz, A., and Wiener, S.I. (2001). Active locomotion increases peak firing rates of anterodorsal thalamic head direction cells. J. Neurophysiol. *86*, 692–702.

STAR★METHODS

KEY RESOURCES TABLE

REAGENT or RESOURCE	SOURCE	IDENTIFIER
Software and algorithms		
Matlab	www.mathworks.com	release 2018a
Other		
Motion platform	www.ckas.com.au	6 DOF platform

RESOURCE AVAILABILITY

Lead contact

Further information and requests for resources should be directed to and will be fulfilled by the lead contact, David Alais (david.alais@sydney.edu.au).

Materials availability

This study did not generate new unique reagents or other materials.

Data and code availability

- The data have been deposited and are publicly available as of the date of publication at OSF https://osf.io/msd8c/

- All original code central to supporting the main claims of the paper has been deposited at https://osf.io/msd8c/ and is publicly available as of the date of publication.

- Any additional information required to reanalyze the data reported in this paper is available from the lead contact upon request.

EXPERIMENTAL MODEL AND SUBJECT DETAILS

Participants

Fourteen adult observers (8 female, 6 male: mean age 20.6 years) participated in Experiment 1 and 10 (6 female, 4 male: mean age 19.7 years) in Experiment 2. All were adults with normal or corrected-to-normal vision and functional stereovision, as tested with the Fly Stereo Acuity Test. All gave informed consent and there were no exclusions: all participants were included in data analyses. Participants were university undergraduates from first and second year with no prior experience in perception experiments and no previous exposure to binocular rivalry. Participants were therefore naive about the aims and hypotheses except for one participant in Experiment 1 (author RK). The experiment was approved by the Human Research Ethics Committee of the University of Sydney. The experimental procedure conformed to the declaration of Helsinki and participants gave informed consent before to commencing the experiment.

METHOD DETAILS

Apparatus

Experiment 1: Passive rotation. A 6 degrees of freedom motion platform (CKAS Mechatronics, Australia: see reference for a full description) was used to rotate observers passively in the yaw plane (Experiment 1: see Figure 1C). The visual stimulus was displayed in an Oculus Rift DK2 head-mounted display (Oculus, Menlo Park, USA) with a refresh rate of 75 Hz and screen resolution of 960 × 1080 pixels per eye. Eye movements were recorded inside the Oculus headset by custom built stereo eye-trackers and the observer's head position was recorded by a Xsens gyroscope (Xsens, Enschede, The Netherlands).

Experiment 2: Active rotation. Observers sat on a pivoting stool wearing a HTC Vive Pro head-mounted display (HTC, New Taipei, Taiwan) which presented the same visual stimulus as in Experiment 1 with a refresh rate of 100 Hz and screen resolution of 960 × 1080 pixels per eye. Headtracking was provided by an integrated head-tracking unit built into the Vive headset.

Stimuli

The visual stimuli in both experiments were two drifting sine-wave gratings with opposite directions of motion, one presented to each eye in corresponding retinal locations. The gratings were either horizontally or vertically opposed, depending on condition, and were displayed within an annulus with an outer radius of 6° of visual angle and an inner radius of 2.5°. The center of the annulus was set to a uniform mean-luminance grey (30.6 cd m^{-2}) and contained a large fixation cross (diameter = 2.2° visual angle). The inner radius was chosen based on piloting that showed a motion-free central blank region of 2.5° of visual angle was large enough to prevent OKN tracking in response to the drifting grating, as confirmed by eye-movement recordings in piloting (see Figure S1). The outer region surrounding the grating was filled with static noise that was matched between the eyes. The spatial frequency and Michelson contrast of the gratings were 0.4 cyc/deg and 75.1%, respectively, and the gratings drifted at a rate of 4 cycles per second (speed = 10°/s). Note that the annular window containing the apertures was in central vision and remained fixed in head-centered coordinates during rotation and that the gratings drifted with a constant retinal velocity at all times (no dependence on head position).

The rotation was the same in both experiments: a sinusoidal oscillation in the yaw plane with an amplitude of $\pm 24°$ and a period of 4 s (0.25 Hz) which continued for 16 cycles (64 s). In the passive experiment, this was provided by the motion platform, and in the active experiment observers self-rotated by rotating their head to follow a rotation guide presented in the head-mounted display that oscillated – in real-world coordinates – through $\pm 24°$ at 0.25 Hz. Head-tracking data confirmed that active and passive rotations were equivalent (see Figures 3E and 3F).

Procedure

Before the start of the experiment, observers adjusted the headset comfortably and then ensured the left- and right-eye images were stably fused by nudging the horizontal position of the two half-images using the left and right arrow keys. Observers then practiced the task, which was to indicate continuously the alternations in perceived direction of the rivalling gratings while maintaining fixation on the central cross. Observers reported perceived direction (either left/right or up/down) by holding down the appropriate key on a keyboard (or a custom-built button box, in Experiment 2) as long as each percept lasted, thereby producing a continuous time series of their alternating perception. There were 4 conditions in a 2 × 2 combination: the rivalling visual motions were either vertically or horizontally opposed, and the observer was either static or rotating in the yaw plane. Observers completed 8 trials per condition (32 trials to complete the experiment), with each trial lasting 64 s and comprising 16 full cycles of sinusoidal oscillation (4 s period, 0.25 Hz).

Experiment 1: The rotation was passively applied by the motion platform while the observer sat in a wrap-around driving seat secured by a seat-belt harness and maintaining steady head position. In a factorial combination, trials beginning with leftward rotation were counterbalanced with rotations beginning rightward, eye and direction of visual motion were counterbalanced (left/right eye receiving leftward/rightward motion vs. left/right eye receiving rightward/leftward motion) and horizontal and vertical grating motion were counterbalanced. The full factorial combination was presented in a randomised order for each participant in a single block of 16 trials. Data was also collected in a no-rotation condition to compare rivalry dynamics without any vestibular input. This was done in a separate block of 16 trials, with a randomised factorial order of conditions similar to the yaw rotation condition except that there was no factor of initial rotation direction. The order of the static and rotation blocks was counterbalanced between observers.

QUANTIFICATION AND STATISTICAL ANALYSIS

The effect of yaw rotation on resolving ambiguous visual motion was studied in four conditions. In Experiment 1, there were two rotation conditions: observers sat on the motion platform and underwent a sinusoidal, horizontal (yaw), whole-body rotation at 0.25 Hz while viewing a pair of rivalling visual motions that were either horizontally or vertically opposed. In the horizontal visual condition, the dichoptic motions were aligned with the trajectory of rotation and in the vertical condition they were orthogonal (Figure 1). In two stationary conditions, observers viewed the same horizontal or vertical motion rivalry while seated on the stationary motion platform. In all conditions, participants tracked their rivalry alternations so that their perceptual dynamics could be compared with the rotation signal. In Experiment 2: the rotation was self-generated by the observer (see Stimuli for details). The procedure and conditions were identical to

Experiment 1 in all respects except that static and rotation trials were not conducted in separate blocks but were randomly interleaved in one large randomised order of 32 trials.

Participants tracked their fluctuations in perceived visual direction over 64-s trials (Figure 1E) and their alternation data for 8 trials in a given condition were averaged (Figure 2A). To avoid potential artefacts due to the platform accelerating/decelerating, the first and last cycles of rotation were trimmed, leaving the middle 56 s (14 cycles) for analysis. To capture the alternations in each participant's data, a sine model was fitted in each condition to their mean data for the 8 tracking trials using Equation 1:

$$f(t) = a\cos(\omega t) + b\sin(\omega t) = A\cos(\omega t + \phi) \qquad \text{(Equation 1)}$$

where t is time, ω is frequency, and a and b are cosine and sine coefficients, respectively. A and Φ represent the amplitude and phase of the sinusoidal fits (as in Figures 2C, 2E, 3A, and 3C), while the coefficients a and b are used when working with circular statistics (as in Figures 2F and 3D). The fitting is carried out with a very fine frequency resolution (steps of 0.001 Hz), making this effectively a continuous first-order Fourier analysis and it has several advantages over using a discrete FFT. The principal benefit is that it provides better estimates of phase and amplitude by avoiding the artefacts of spectral smear ('leakage') and loss of power at the fundamental frequency ('scalloping') that commonly arise when using FFTs (Lyons, 2011).

Curve fitting was done using the restricted maximum likelihood method implemented in R and goodness-of-fit (R^2) was computed to measure the agreement between the model and the data. Rather than relying on a single best-estimate of frequency, we fitted all frequencies over a broad range of interest (0.14 – 0.50 Hz; periods of 2–7 s) in steps of 0.001 Hz to obtain the clearest picture of frequency selectivity and to check for possible harmonics or other prominent frequencies. The frequency range used for analysis was chosen before the experiment based on piloting and ranged from approximately half the rotation rate of 0.25 Hz to twice the rate, and mean alternation rates in the experimental data were all contained within this range. At each step in the frequency range, frequency was fixed at that value and amplitude and phase free to vary. For each subject, we fitted the best sinusoid (at a given frequency level) to the data of each individual trial and calculated the mean R^2 of the fits to the eight trials. This was repeated at each level of fitted frequency to produce a function of R^2 values over frequency for each individual participant, as shown by the thin lines in Figures 2C, 2D, 3A, and 3B.

The single-cycle data in Figures 2E and 3C were obtained using group mean data. First, all the tracking data (10 [or 14] observers × 8 trials) were averaged into a group mean trial and a 0.25-Hz sinusoid was fitted as described above. To illustrate a single cycle, the data were divided into 4-s periods, combined into an average and then overlaid with a single cycle of the sinusoid. Because the single-cycle plots were designed to test how well the perceptual alternation data conform to a sinusoidal pattern with a 4-s period, they are plotted with no phase offset – even though phase and amplitude both varied in the fitting process. The plots contain 240 data points per condition (4 s of data at a sampling rate of 60 Hz), with each point being the mean over all trials and observers and over the 14 pooled cycles.

The polar plots shown in Figures 2F and 3D contain vectors calculated using circular statistics based on the cosine and sine weights obtained from the curve-fitting procedure (Equation 1). Every trial is represented in the plots (10 [or 14] observers × 8 trials), with each vector showing the amplitude and phase of a single trial. The arrow shows the phase of the resultant vector when all trials are combined, and shading around the arrow shows the 95% confidence interval generated by 10,000 iterations of bootstrapping the trials and recomputing the group mean resultant. The mean phases compared in Figure 4B are taken from the polar plots.